Reaction Kinetics and Mechanism of Magnetic Field Effect in Cryptochrome (Supporting Material)

Ilia A. Solov'yov[*,†] and Klaus Schulten[*,†,‡]

Beckman Institute for Advanced Science and Technology, University of Illinois at Urbana-Champaign, Urbana, Illinois, USA, and Department of Physics, University of Illinois at Urbana-Champaign, Urbana, Illinois, USA

E-mail: ilia@illinois.edu; kschulte@ks.uiuc.edu

[*]To whom correspondence should be addressed
[†]Beckman Institute, University of Illinois at Urbana-Champaign
[‡]Department of Physics, University of Illinois at Urbana-Champaign

Absorption spectrum

The efficiency of light absorption at wavelength λ by an absorbing medium is characterized through the absorbance $A(\lambda)$ defined as[1]

$$A(\lambda) = \log \frac{I_0(\lambda)}{I(\lambda)}, \tag{S1}$$

where $I_0(\lambda)$ and $I(\lambda)$ are the light intensities of the beam entering and leaving the absorbing medium, respectively. According to the reaction scheme in Fig. 2, cryptochrome can occupy several states, which are expected to absorb light differently. Therefore, according to the Beer-Lambert-Bouguer law,[1] the absorbance of the cryptochrome-containing sample is given by Eq. (1).

The molar extinction coefficient, ε_i, in Eq. (1) of a light-absorbing component in the system is directly related to the absorption cross section, σ_i, which characterizes the photon-capture area of a molecule[1]

$$\sigma_i(\lambda) = 1000 \ln(10) \frac{\varepsilon_i(\lambda)}{N_A} = 3.82 \times 10^{-21} \varepsilon_i(\lambda). \tag{S2}$$

Here N_A is Avogadro's number; the absorption cross section in Eq. (S2) is measured in units of cm^2.

Rate constants

The rate constants in Eqs. (2)-(10) determine the time evolution of intermediate states in cryptochrome. Many of the rate constants are available from experiments performed on cryptochrome and cryptochrome-like proteins from various species, such as garden warbler,[2] *Drosophila melanogaster*,[3,4] *Arabidopsis thaliana*,[5,6] and *Homo sapiens*.[4,7] Many studies were also done for DNA photolyase, a protein structurally similar to cryptochrome.[8–11,11–13] Some of the rate constants can be independently estimated from fundamental physical principles.[14,15] The adopted rate constants are summarized in Tab. 1.

Flavin photoexcitation. The rate constants k_1 and k_2 represent the rate of photoexcitation of the flavin cofactor from its fully oxidized FAD state and from the semiquinone $FADH^{\bullet}$ state to the excited FAD^{*} and $FADH^{\bullet *}$ states, respectively, (see Fig. 2). The $FAD \rightarrow FAD^{*}$ and $FADH^{\bullet} \rightarrow FADH^{\bullet *}$ transitions are induced by a laser pulse (see Fig. 1) and arise only during the pulse duration τ. The rate constants k_1 and k_2 depend on the laser power and can be estimated as

$$k_{ex} = \sigma \frac{P\chi}{E_{ph} S_0} \left(1 - \Theta(t-\tau)\right), \tag{S3}$$

where $P = E/\tau$ is the power of the laser pulse (with E being the energy of the pulse and τ the pulse duration), S_0 is the cross section area of the light beam hitting the sample, $\chi \leq 1$ defines the fraction of power deposited at the sample, σ is the absorption cross section defined in Eq. (S2), $E_{ph} = hc/\lambda$ is the energy of a single photon (with h being the Planck constant and c the speed of light), $\Theta(x)$ is the Heaviside step-function which limits the photoexcitation of FAD and $FADH^{\bullet}$ to the period of the laser pulse duration. Here we do not consider the periodicity of the laser pulses as the time interval between two successive pulses is significantly longer than the typical reaction times involved in the scheme shown in Fig. 2 (the pulse frequency used in the observation[2] was 10 Hz).

Assuming a Gaussian radial profile of the laser beam and substituting Eq. (S2) into Eq. (S3) one obtains

$$k_{ex} = 612.686 \times \frac{P\lambda\varepsilon(\lambda)}{R^2} \left[\frac{1 - \exp\left(-R^2/\omega^2\right)}{1 - \exp\left(-R_0^2/\omega^2\right)}\right] \left(1 - \Theta(t-\tau)\right), \tag{S4}$$

where R is the radius of the beam at the sample measured in μm, R_0 is the radius of the output beam from the laser measured in μm and ω is the radius at which the laser field amplitude drops to $1/e$. ε in Eq. (S4) is measured in $\mathrm{L \cdot mol^{-1} cm^{-1}}$, λ is measured in nm and P is measured in Watt.

In the measurements[2] the R_0 value was $R_0 = 3000$ μm and the size of the sample used was likely smaller allowing one to assume $R = 1500$ μm. With $\omega = 1000$ μm, a typical value for the amplitude fall-off of the laser beam,[16,17] Eq. (S4) can be used to estimate the photoexcitation rate

constants k_1 and k_2. The rate constants k_1 and k_2 are determined by the laser wavelength, 355 nm, and the beam power, 10^6 W.[2] Figure S1 shows that the extinction coefficient of the oxidized flavin (FAD) at $\lambda = 355$ nm is about 7900 $\mathrm{L \cdot mol^{-1} cm^{-1}}$,[2,13] resulting in $k_1 = 6.8 \times 10^8$ $\mathrm{s^{-1}}$. The absorption (extinction) spectra in Fig. S1 were recorded for the three redox states of FAD[18] and normalized to the absorption of FAD at 450 nm ($\varepsilon_{450} = 11.3 \times 10^4$ $\mathrm{L \cdot mol^{-1} cm^{-1}}$) (solid line).[2] We note that the wavelength dependence of the extinction coefficient in garden warbler,[2] Drosophila, and human[3,7] cryptochromes maintains the general features of the absorption profile shown in Fig. S1. Similarly, Fig. S1 shows that the extinction coefficient of semiquinone ($\mathrm{FADH^{\bullet}}$) flavin at $\lambda = 355$ nm is about 10400 $\mathrm{L \cdot mol^{-1} cm^{-1}}$ (solid line),[2,13] resulting in $k_2 = 9 \times 10^8$ $\mathrm{s^{-1}}$. The rate constants k_1 and k_2 apply only during the laser pulse duration time of $\tau = 5$ ns.

Flavin excited states relaxation. The rate constants $k_{rel}^{(1)}$ and $k_{rel}^{(2)}$ describe the $\mathrm{FAD^*} \rightarrow \mathrm{FAD}$ and $\mathrm{FADH^{\bullet *}} \rightarrow \mathrm{FADH^{\bullet}}$ relaxation processes, respectively (see Fig. 2). These relaxation processes have not been very well documented in cryptochrome, but the $\mathrm{FADH^{\bullet *}} \rightarrow \mathrm{FADH^{\bullet}}$ transition was studied in DNA photolyase,[9] a protein homologous to cryptochrome.[19,20] According to experimental measurement[9] the lifetime for the relaxation of $\mathrm{FADH^{\bullet *}}$ to the ground state is 80 ps, leading to the value $k_{rel}^{(2)} = 1.25 \times 10^{10}$ $\mathrm{s^{-1}}$. The $\mathrm{FAD^*} \rightarrow \mathrm{FAD}$ transition is expected to occur on a similar timescale and, accordingly, we assume $k_{rel}^{(1)} = 1.25 \times 10^{10}$ $\mathrm{s^{-1}}$.

Radical pair formation. The rate constant k_{rp} describes the $^1[\mathrm{FADH^{\bullet}} + \mathrm{Trp^{\bullet}}]$ radical pair formation process (see Fig. 2). The characteristic time for this process is 30 ps, as confirmed by using ultrafast pump-probe spectroscopy in the near-infrared spectral region in DNA photolyase,[11] leading to $k_{rp} = 3.3 \times 10^{10}$ $\mathrm{s^{-1}}$. Although k_{rp} has not been clearly resolved for cryptochrome, we assume the rate constant from DNA photolyase to be of the same order of magnitude in all photolyase/cryptochrome-like proteins.[7,8,14]

Flavin deprotonation. The rate constant $k_{ox}^{(1)}$ describes the deprotonation process of $\mathrm{FADH^+}$, as denoted in Fig 2. Since the $\mathrm{FADH^+}$ state of the flavin cofactor has never been observed in

cryptochrome, and/or photolyase,[2,4–11,11,12,21] the characteristic time of $FADH^+$ deprotonation is expected to be on the order of few picoseconds, which is beyond experimental resolution. Thus, we assume the value $k_{ox}^{(1)} = 1/10\ \text{ps} = 10^{11}\ \text{s}^{-1}$.

Electron transfer involving flavin radical. The rate constants $k_{et}^{(1)}$ describes electron transfer from the $FADH^\bullet$ radical to the $Trp^\bullet$ radical (see Fig. 2). $k_{et}^{(1)}$ is expected to have an approximate value of $1/10\ \mu\text{s} = 10^5\ \text{s}^{-1}$, since the radical pair in cryptochrome is assumed to have a lifetime of 6 μs;[7] measurements were performed using transient EPR spectroscopy, with the system optically excited by a Nd:YAG laser (Spectra Physics GCR-11) pumping an optical parametric oscillator (Opta BBO-355-vis/IR, Opta GmbH, Bensheim, Germany) tuned to a wavelength of 460 nm (pulse width 6 ns; pulse energy 4 mJ). At this particular wavelength the extinction coefficient of the semiquinone ($FADH^\bullet$) flavin is about 3600 $\text{L}\cdot\text{mol}^{-1}\text{cm}^{-1}$ (see blue solid line in Fig. S1). The chosen laser pulse power leads to the photoexcitation rate constant $k_2 = 2.6\times10^8\ \text{s}^{-1}$ under the assumption that the geometrical characteristics of the laser beams in two experiments[2,7] are identical. Since the fast photoexcitation decay channel of the radical pair is only possible during the period of the laser pulse, the fourfold decrease of the photoexcitation rate constant would lead to a significant increase of the lifetime of the radical pair state allowing its detection in the EPR measurements.

The rate constant $k_{et}^{(2)}$ describes electron transfer from the $Trp^\bullet$ radical to the excited $FADH^{\bullet *}$ radical. The electron transfer rate constant for this process was measured in DNA photolyase using time-resolved absorption spectroscopy and found to be $k_{et}^{(2)} = 2.6\times10^{10}\ \text{s}^{-1}$.[9] Similar values for the electron transfer rate constants can also be estimated from Marcus theory of electron transfer.[14]

S $\leftrightarrow$ T interconversion. The rate constant k_{sf} describes the singlet-triplet interconversion process in cryptochrome (see Fig. 2) as a first order reaction process. We employ such process as a very rough model for the actual quantum mechanical spin precession process, since only time scale and yield of singlet-triplet interconversion matter. The k_{sf} rate constant depends on several factors, such as the hyperfine interaction in the radical pair, exchange and dipole-dipole interaction between

the radical pair partners, and the external magnetic field. To calculate the singlet-triplet kinetics one needs to solve the stochastic Liouville equation for the radical pair in the system.[14,15,22,23] In the present study we cast the transition process into a single rate constant as done earlier.[24] It has been demonstrated[14,15,25] that for a generic radical pair holds $k_{sf} = 10^6 - 10^8$ s^{-1}. k_{sf} is magnetic field dependent and, thereby, responsible for the magnetic field effect in cryptochrome. We demonstrate the feasibility of a magnetic field effect in cryptochrome by varying the value of k_{sf}. If cryptochrome is the primary magnetoreceptor protein in birds and other animals, it is natural to assume that nature has designed it in such a way that the external geomagnetic field produces a significant effect. The time needed for a significant transformation of a singlet state $^1[\mathrm{FADH}^\bullet + \mathrm{Trp}^\bullet]$ into a triplet state $^3[\mathrm{FADH}^\bullet + \mathrm{Trp}^\bullet]$ and vice versa in a 0.5 G magnetic field is typically ~ 700 ns;[25] therefore we assume $k_{sf} = 10^6$ s^{-1} for the singlet-triplet interconversion rate constant.

Singlet and Triplet decay kinetics. The rate constants k_S and k_T describe the singlet and the triplet decays of the $[\mathrm{FADH}^\bullet + \mathrm{Trp}^\bullet]$ radical pair (see Fig. 2). Together with the $k_{et}^{(1)}$ electron transfer rate constant they define the lifetime of the radical pair. According to the experiment, the lifetime of the radical pair in cryptochrome is $\gtrsim 6\ \mu$s;[7] therefore, we assume $k_S = k_T = 1/10\ \mu\mathrm{s} = 10^5$ s^{-1}, i.e. we take the lower bound as our estimate of the radical pair lifetime. For the sake of simplicity we also assume spin-independent decay kinetics of the radical pair, i.e. $k_S = k_T$.

Dark reaction kinetics. The rate constants k_{red} and $k_{ox}^{(2)}$ are associated with the two-step cryptochrome dark reaction (see Fig. 2). Both stages involved are expected to be fairly long-lived, with a lifetime on the order of milliseconds, and should be resolved in transient absorption spectra reported in the experiment.[2] According to the experiment, two transient states in cryptochrome with lifetimes of 4 ms and 14 ms were detected. k_{red} describes the reduction process of the semiquinone $\mathrm{FADH}^\bullet$ radical possibly involving the $\mathrm{O}_2^{\bullet-}$ radical, as suggested earlier.[15] It is natural to expect that the lifetime of the signalling state in cryptochrome is maximal, leading to the values $k_{red} = 1/14$ ms ≈ 70 s^{-1} and $k_{ox}^{(2)} = 1/4$ ms $= 250$ s^{-1}.

Flavin absorption spectra

Optical absorbance of cryptochrome is dominated by the absorbance of the isoalloxazine moiety in FAD.[2,7] Figure S1 shows absorption spectra recorded for the three redox states of FAD: the fully reduced $FADH^-$, one-electron oxidized $FADH^\bullet$ and the two-electron oxidized FAD.[7,18,26]

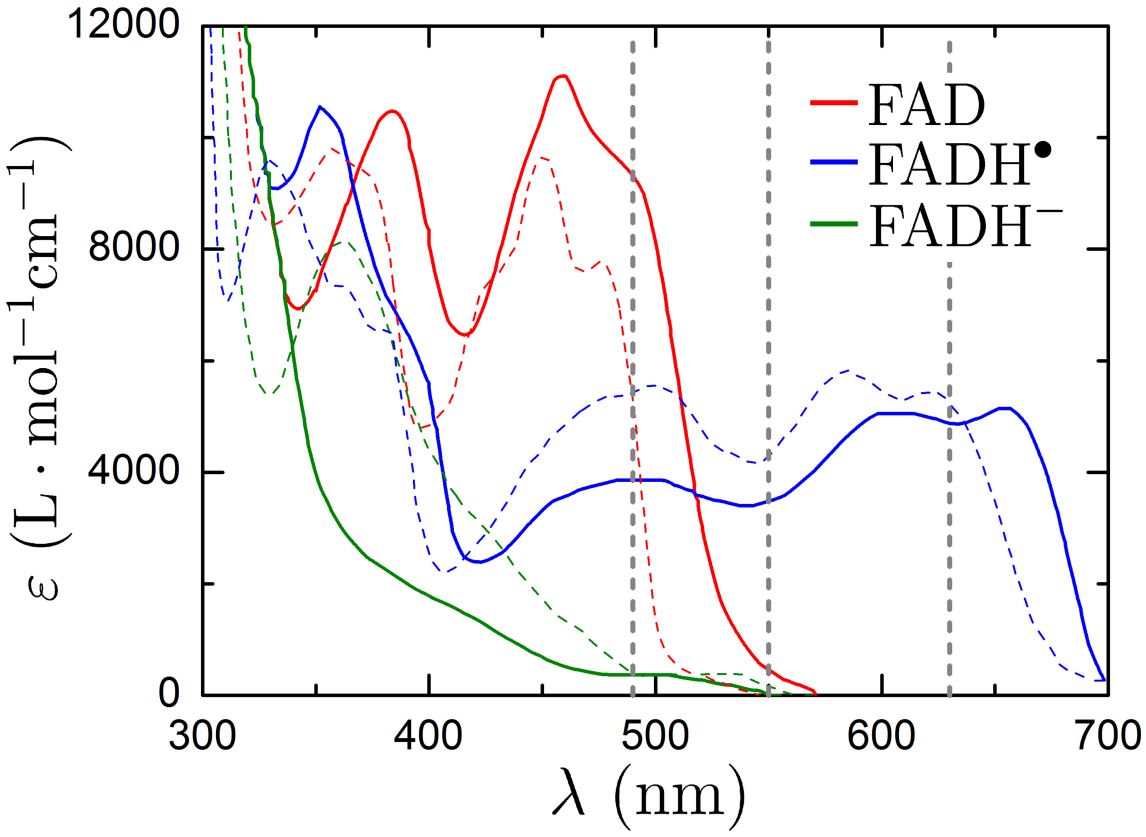

Figure S1: **Flavin absorption spectra.** Wavelength dependence of the molar absorption of the flavin chromophore in its three redox states FAD (red line), $FADH^\bullet$ (blue line), and $FADH^-$ (green line). Vertical dashed lines set the limits for the wavelengths used in experiment[2] and in the calculations reported here. The spectra of the flavin chromophore shown as a solid line have been adopted from a textbook,[18] while the spectra of different redox forms of selected cryptochrome/photolyase shown as a dashed line are digitized from the measured pattern.[26]

The calculated absorption spectrum in Fig. 3 depends on the value of the extinction coefficients, ε_i, of the cryptochrome transient states (see Eq. (1)), which are wavelength dependent. The extinction coefficients for FAD, $FADH^\bullet$ and $FADH^-$ were chosen as 300 $L \cdot mol^{-1}cm^{-1}$,

2695 $\mathrm{L \cdot mol^{-1} cm^{-1}}$ and 690 $\mathrm{L \cdot mol^{-1} cm^{-1}}$, respectively, for 490-550 nm, and the extinction coefficient for $\mathrm{FADH^{\bullet}}$ at 550-630 nm was assumed to be 3843 $\mathrm{L \cdot mol^{-1} cm^{-1}}$. Figure S1 illustrates that the chosen values are consistent with the experimentally recorded absorption profiles for the different redox states of the flavin moiety.

The only noticeable difference between calculated and observed spectra is the increased value of the extinction coefficient for the fully reduced $\mathrm{FADH^{-}}$ state of the flavin cofactor, which in the calculation is slightly larger than the extinction coefficient for the fully oxidized FAD state. However, both extinction coefficients are expected to be small (see Fig. S1), as they are taken from the far edge of the absorption spectrum. Therefore, the inaccuracy in their value is high, but inconsequential. To illustrate the uncertainty of flavin extinction at 490-550 nm in Fig. S1 we show two sets of absorption profiles for the different redox states of the flavin cofactor recorded for an isolated flavin cromophore[18] (solid line) and for the selected cryptochrome/photolyase proteins[26] (dashed line). Although in both systems the absorption spectra contain similar features, one notes that the spectra for the oxidized (FAD) and semiquinone ($\mathrm{FADH^{\bullet}}$) states in the isolated flavin chromophore are red-shifted with respect to the spectra recorded for cryptochrome/photolyase proteins, thereby exhibiting significantly different absorption at 490-550 nm. Another reason for the increased absorption of the $\mathrm{FADH^{\bullet}}$ state in our model may be that in the experiment[2] $\mathrm{FADH^{-}}$ is actually substituted by the anionic $\mathrm{FAD^{\bullet -}}$ radical state which exhibits a somewhat higher absorption at 490-550 nm.[26] This explanation is worth studying in a systematic fashion.

Transient absorption is a powerful technique for studying intermediate states in chemical reactions, but the method often delivers data which cannot be unequivocally interpreted since the absorption patterns for different molecules and their various states often overlap. The impact of simultaneous absorption of several transient states at the same wavelength on the total absorption of the sample had to be addressed already three decades ago for pyrene/DMDMA complex,[24] where a theoretical approach, similar to the method which we now use for cryptochrome transient absorption calculation, was successfully employed in the first quantitative demonstration of a radical pair magnetic field effect. Large biomolecules usually have many constituents which respond to

the typical wavelengths used by probe light in the transient absorption experiment. Recent studies on transient absorption of cryptochrome, and cryptochrome-like proteins, often deliver a single explanation for the measured data and do not discuss how the result would change if other possible transient states of the studied proteins were taken into account. The only way to unequivocally interpret the results of measurements in the present case is through measurements at different conditions that likely impact the reaction kinetics and shift the equilibrium toward different transient states.

References

(1) Lakowicz, J. R. *Limological Analysis*; Springer, New York, 2006.

(2) Liedvogel, M.; Maeda, K.; Henbest, K.; Schleicher, E.; Simon, T.; Timmel, C. R.; Hore, P.; Mouritsen, H. *PLoS ONE* **2007**, *2*, e1106.

(3) Shirdel, J.; Zirak, P.; Penzkofer, A.; Breitkreuz, H.; Wolf, E. *Chem. Phys.* **2008**, *352*, 35–47.

(4) Hoang, N.; Schleicher, E.; Kacprzak, S.; Bouly, J.-P.; Picot, M.; Wu, W.; Berndt, A.; Wolf, E.; Bittl, R.; Ahmad, M. *PLoS Biol.* **2008**, *6*, 1559–1569.

(5) Bouly, J.-P.; Schleicher, E.; Dionisio-Sese, M.; Vandenbussche, F.; Van Der Straeten, D.; Bakrim, N.; Meier, S.; Batschauer, A.; Galland, P.; Bittl, R.; Ahmad, M. *J. Biol. Chem.* **2007**, *282*, 9383–9391.

(6) Giovani, B.; Byrdin, M.; Ahmad, M.; Brettel, K. *Nat. Struct. Biol.* **2003**, *10*, 489–490.

(7) Biskup, T.; Schleicher, E.; Okafuji, A.; Link, G.; Hitomi, K.; Getzoff, E. D.; Weber, S. *Angew. Chem. Int. Ed. Engl.* **2009**, *48*, 404–407.

(8) Henbest, K. B.; Maeda, K.; Hore, P. J.; Joshi, M.; Bacher, A.; Bittl, R.; Weber, S.; Timmel, C. R.; Schleicher, E. *Proc. Natl. Acad. Sci. USA* **2008**, *105*, 14395–14399.

(9) Byrdin, M.; Eker, A. P.; Vos, M. H.; Brettel, K. *Proc. Natl. Acad. Sci. USA* **2003**, *100*, 8676–8681.

(10) Kao, Y.-T.; Tan, C.; Song, S.-H.; Öztürk, N.; Li, J.; Wang, L.; Sancar, A.; Zhong, D. *J. Am. Chem. Soc.* **2008**, *130*, 7695–7701.

(11) Aubert, C.; Vos, M. H.; Mathis, P.; Eker, A. P.; Brettel, K. *Nature* **2000**, *405*, 586–590.

(12) Gindt, Y. M.; Vollenbroek, E.; Westphal, K.; Sackett, H.; Sancar, A.; Babcock, G. T. *Biochem.* **1999**, *38*, 3857–3866.

(13) Prytkova, T. R.; Beratan, D. N.; Skourtis, S. S. *Proc. Natl. Acad. Sci. USA* **2007**, *104*, 802–807.

(14) Solov'yov, I. A.; Chandler, D.; Schulten, K. *Biophys. J.* **2007**, *92*, 2711–2726.

(15) Solov'yov, I. A.; Schulten, K. *Biophys. J.* **2009**, *96*, 4804–4813.

(16) Bartels, A.; Hudert, A.; Janke, C.; Dekorsy, T.; Köhler, K. *Appl. Phys. Lett.* **2006**, *88*, 04117–(1–3).

(17) Berera, R.; van Grondelle, R.; Kennis, J. T. M. *Photosynth. Res.* **2009**, *101*, 105–118.

(18) Schmidt, W. *Optical Spectroscopy in Chemistry and Life Sciences, an Introduction*; Wiley-VCH, 2005.

(19) Brautigam, C. A.; Smith, B. S.; Ma, Z.; Palnitkar, M.; Tomchick, D. R.; Machius, M.; Deisenhofer, J. *Proc. Natl. Acad. Sci. USA* **2004**, *101*, 12142–12147.

(20) Lin, C.; Shalitin, D. *Annu. Rev. Plant Biol.* **2003**, *54*, 469–496.

(21) Ritz, T.; Yoshii, T.; Helfrich-Foerster, C.; Ahmad, M. *Commun. & Integr. Biol.* **2010**, *3*, 21–27.

(22) Cintolesi, F.; Ritz, T.; Kay, C.; Timmel, C.; Hore, P. *Chem. Phys.* **2003**, *294*, 707–718.

(23) Efimova, O.; Hore, P. *Biophys. J.* **2008**, *94*, 1565–1574.

(24) Schulten, K.; Staerk, H.; Weller, A.; Werner, H.-J.; Nickel, B. *Z. Phys. Chem.* **1976**, *NF101*, 371–390.

(25) Rodgers, C. T.; Hore, P. J. *Proc. Natl. Acad. Sci. USA* **2009**, *106*, 353–360.

(26) Liu, B.; Liu, H.; Zhong, D.; Lin, C. *Cur. Opin. Plant Biol.* **2010**, *13*, 578–586.